



Open Archive TOULOUSE Archive Ouverte (OATAO)

OATAO is an open access repository that collects the work of Toulouse researchers and makes it freely available over the web where possible.

This is an author-deposited version published in : <http://oatao.univ-toulouse.fr/>
Eprints ID : 4729

To link to this article : DOI :10.1063/1.3348795
URL : <http://dx.doi.org/10.1063/1.3348795>

To cite this version : Mehdaoui, B. and Meffre, A. and Lacroix, L.-M. and Carrey, J. and Lachaize, S. and Respaud, M. and Gougeon, M. and Chaudret, Bruno (2010) *Magnetic anisotropy determination and magnetic hyperthermia properties of small Fe nanoparticles in the superparamagnetic regime*. Journal of Applied Physics, vol. 107 (n° 9). ISSN 0021-8979

Any correspondence concerning this service should be sent to the repository administrator: staff-oatao@inp-toulouse.fr.

Magnetic anisotropy determination and magnetic hyperthermia properties of small Fe nanoparticles in the superparamagnetic regime

B. Mehdaoui,¹ A. Meffre,¹ L.-M. Lacroix,¹ J. Carrey,^{1,a)} S. Lachaize,¹ M. Respaud,¹ M. Gougeon,² and B. Chaudret³

¹Université de Toulouse; INSA; UPS; Laboratoire de Physique et Chimie des Nano-Objets (LPCNO), 135 Avenue de Rangueil, F-31077 Toulouse, France and CNRS; UMR 5215; LPCNO, F-31077 Toulouse, France

²Institut CARNOT-CIRIMAT-UMR 5085, Bâtiment 2R1, 118 route de Narbonne, F-31062 Toulouse, France

³Laboratoire de Chimie de Coordination-CNRS, 205 route de Narbonne, 31077 Toulouse Cedex 4, France

We report on the magnetic and hyperthermia properties of 5.5 nm in diameter iron nanoparticles synthesized by organometallic chemistry, which display the bulk magnetization. Quantitative analysis of alternative susceptibility measurements allows the determination of the effective anisotropy $K_{\text{eff}}=1.3 \times 10^5 \text{ J m}^{-3}$. Hyperthermia measurements are performed at a magnetic field up to 66 mT and at frequencies in the range of 5–300 kHz. Maximum measured specific absorption rate (SAR) is 280 W/g. SAR displays a square dependence with the magnetic field below 30 mT but deviates from this power law at higher value. SAR is linear with the applied frequency for $\mu_0 H = 19 \text{ mT}$. These results are discussed in the light of linear response theory.

I. INTRODUCTION

Magnetic nanoparticles (MNPs) are of particular interest for biomedical application such as single molecule detection,¹ drug release,² or magnetic hyperthermia treatment.³ In order to lower the detection limit or to provide an important temperature increase, all these applications require MNPs with a high magnetic moment.⁴ Therefore, the widely used iron oxide particles, such as maghemite ($\gamma\text{-Fe}_2\text{O}_3$, $80 \text{ A m}^2 \text{ kg}^{-1}$) or magnetite (Fe_3O_4 , $120 \text{ A m}^2 \text{ kg}^{-1}$), could be advantageously replaced by metallic particles such as cobalt (Co, $160 \text{ A m}^2 \text{ kg}^{-1}$), iron (Fe, $220 \text{ A m}^2 \text{ kg}^{-1}$), or iron cobalt alloy (FeCo, $240 \text{ A m}^2 \text{ kg}^{-1}$).

Moreover, for hyperthermia, their size must be optimized to maximize the specific absorption rate (SAR). The optimal size strongly depends on their magnetic anisotropy since both size and anisotropy directly influence their coercive field.⁵ Accurate measurement of the magnetic anisotropy of MNPs is not trivial. One possibility is the precise alternative susceptibility characterizations on well diluted assemblies of magnetically independent NPs.

Our group has developed an organometallic synthesis, allowing the controlled growth of pure metallic iron NPs that display the bulk magnetization.^{6–8} So far, only the determination of the magnetic anisotropy of 1.5 nm in diameter MNPs has been determined and was found equal to $5.2 \times 10^5 \text{ J/m}^3$, i.e., ten times the bulk value.⁹ In this article, we perform a first step toward bigger NPs by the careful study of 5.5 nm NPs, displaying a magnetization close to the bulk one. Hyperthermia measurements as a function of the magnetic field and of the applied frequency have been performed

on samples in which the NPs are in strong magnetic interactions. These results are discussed in the light of linear response theory.

II. RESULTS

Iron NPs exhibiting a polycrystalline bcc structure were synthesized by an organometallic approach in mesitylene solvent.⁷ The resulting “raw” solution is composed of both isolated 5.5 nm NPs and of micrometric agglomerates, as evidenced by both transmission electron microscopy (TEM) micrographs [see Fig. 1(a)] and in dynamic light scattering (DLS) measurements [see Fig. 1(c)]. The size of the NPs inside the agglomerates is roughly the same as the one of the isolated NPs. These aggregates can be removed from the colloidal solution using a standard centrifugation process (20 min at 25 000 rpm). In order to prevent any oxidation, the samples were always kept under an Ar atmosphere. After centrifugation, the supernatant contains only dispersed NPs as evidenced by the DLS results [see Fig. 1(d)]. A single hydrodynamic size distribution is then observed, centered at 8 nm, which is in good agreement with the mean diameter of the particles and their surrounding C_{16} surfactants. This result is confirmed by susceptibility measurements on the raw solution and on the supernatant, following a zero field cooling (ZFC)/field cooling (FC) procedure [see Figs. 1(e) and 1(f)]. The ZFC curve on the raw solution reveals two broad maxima which can be seen as the signature of (i) dispersed NPs with a blocking temperature (T_B) of 30 K and (ii) aggregates of MNPs in which dipolar interactions took place ($T_B=136 \text{ K}$). On the other hand, a unique maximum at 31 K remains in the ZFC of the supernatant after centrifugation. In this case, the magnetic susceptibility follows a Curie–Weiss law $\chi \propto (T - \theta)^{-1}$ for $T > T_B$, with $\theta = -5.0 \text{ K}$ (not shown).

^{a)}Electronic mail: julian.carrey@insa-toulouse.fr.

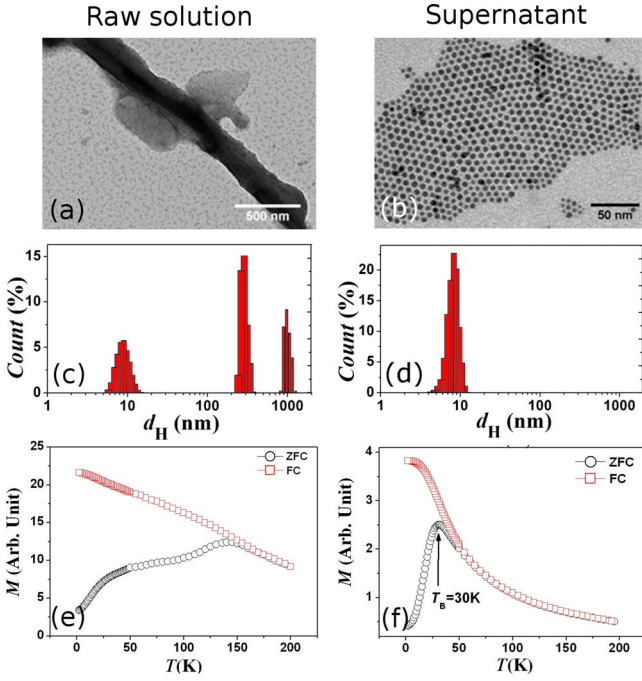


FIG. 1. (Color online) [(a) and (b)] TEM micrographs, [(c) and (d)] hydrodynamic size distribution extracted from DLS measurements, and [(e) and (f)] dc magnetic susceptibility (ZFC-FC) measurements. (a), (c), and (e) correspond to raw solutions and (b), (d), and (f) correspond to centrifugated NPs.

The saturation magnetization (M_S) measured at 2 K for both types of NPs ($M_S = 207 \text{ A m}^2 \text{ kg}^{-1}$) is close to the bulk iron magnetization, i.e., $212 \text{ A m}^2 \text{ kg}^{-1}$ (data not shown here). Moreover, the remnant magnetization (M_R) increases from 41% to 50% of M_S after the centrifugation process, which is the expected value predicted by the Stoner–Wohlfarth theory for noninteracting particles.¹⁰

Frequency dependent susceptibility measurements χ_{ac} were performed on this colloidal solution. The temperature dependence of the in-phase (χ') and the out-of-phase (χ'') components of the susceptibility was measured for frequencies ranging from 0.1 to 1500 Hz. Figure 2 displays the experimental data and the fitting using Gittleman's model,¹¹

$$\bar{\chi}(T, \omega) = \frac{\int_0^\infty \tilde{\chi}_V(T, \omega) v f(v) dv}{\int_0^\infty v f(v) dv} \quad (1)$$

with $\tilde{\chi}_V(T, \omega) = [\chi_S(T) + i\omega\tau\chi_b(T)] / [1 + i\omega\tau]$. $\chi_S = \mu_0 M_S^2(T) v / 3k_B T$ and $\chi_b = \mu_0 M_S^2(T) / 3K_{\text{eff}}$ are, respectively, the contributions from superparamagnetic and blocked NPs. While the saturation magnetization has been fixed according to the magnetization measurements, the other parameters, such as the log normal size distribution $f(v)$ characterized by the mean volume v and its width σ , the relaxing time τ_0 , and the effective anisotropy constant K_{eff} are extracted from the χ_{ac} curves. Their values are summarized in Table I.

Magnetic hyperthermia has been measured as a function of the applied magnetic field amplitude and frequency on a concentrated solution of the raw NPs. For frequencies up to 100 kHz, hyperthermia experiments were performed on a homemade frequency-adjustable electromagnet with a magnetic field ranging up to 30 mT.¹² For $f = 300 \text{ kHz}$, the mea-

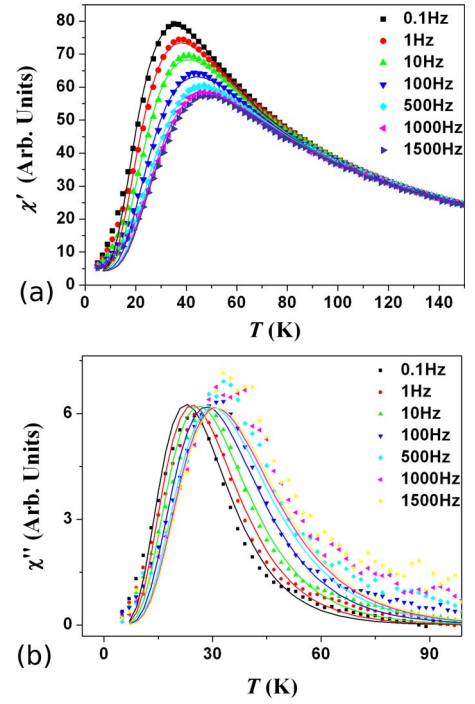


FIG. 2. (Color online) Temperature dependence of the (a) in-phase (χ') and (b) out-of-phase (χ'') components of the alternative susceptibility for varying frequencies. Symbols represent experimental data, and lines are the fits from Gittleman's model using the parameters shown in Table I.

surements were performed on an induction oven, working at a fixed frequency and a maximum magnetic field of 66 mT. An ampoule containing the colloidal solution was sealed under vacuum to prevent any oxidation of the NPs. The ampoule was placed in a calorimeter with 1.5 ml of water, the temperature of which is measured. More details on the measurement method are reported in Ref. 5.

Figure 3(a) displays the SAR measured as a function of the magnetic field in the range of 0–30 mT at frequencies of 50, 100, and 300 kHz. At low field, the SAR shows a square dependence versus the magnetic field, in agreement with the linear response theory (LRT) for superparamagnetic particles. Figure 3(b) displays the SAR values measured at 300 kHz as a function of the applied magnetic in the range of 0–66 mT. For a field above 30 mT, the SAR increases sharply with increasing field and is fitted by a power law function $\text{SAR} \sim H^{3.2}$. The SAR measured at 66 mT is 280 W/g. Figure 3(c) displays the frequency dependence of the SAR at $\mu_0 H = 19.3 \text{ mT}$. A linear dependence of SAR as a function of the frequency was observed.

III. DISCUSSION

Although the aggregates, composed of NPs under strong dipolar interactions, are efficiently precipitated out by the

TABLE I. Adjustment parameters extracted from the fitting of the experimental χ_{ac} curves with Gittleman's model.

d_{moy} (nm)	Distribution	M_S ($\text{A m}^2 \text{ kg}^{-1}$)	τ_0 (s)	K_{eff} (J m^{-3})
5.1	Log normal $\sigma = 0.138$	207	10^{-15}	1.3×10^5

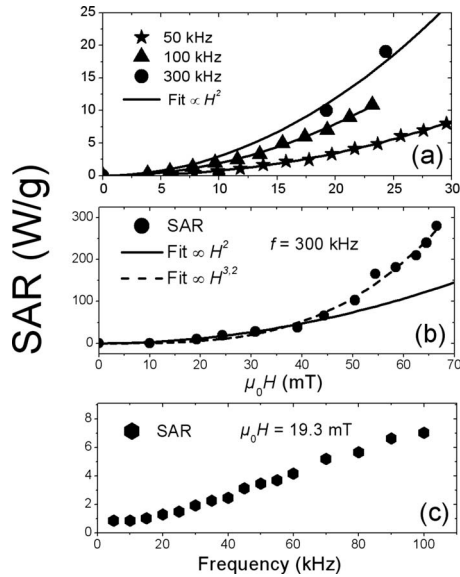


FIG. 3. (a) SAR as a function of magnetic field in the range of 0–30 mT, measured at $f=50, 100,$ and 300 kHz, fitted using $\text{SAR} \sim H^2$. (b) SAR as a function of magnetic field in the range of 0–66 mT, measured at $f=300$ kHz, fitted using $\text{SAR} \sim H^2$ and $H^{3.2}$. (c) Evolution the SAR as a function of frequency, measured at $\mu_0 H=19.3$ mT.

centrifugation process, the NPs remaining in the colloidal solution still interact with each other. These interactions are relatively weak ($\theta=5$ K) and do not affect the hysteresis cycle feature ($M_R/M_S=0.5$). However, they drastically influence the dynamical properties, leading to a very short intrawell relaxation time of $\tau_0=10^{-15}$ s. Such a low value, compared to the usually reported ones (10^{-9} – 10^{-10} s) for individual NP, is consistent with previous experiments on interacting NPs reported by Dorman *et al.*¹³ The fitting of the χ_{ac} using the M_S value ($207 \text{ A m}^2 \text{ kg}^{-1}$) deduced from magnetization measurement gives an estimate of the mean diameter (5.1 nm) in agreement with the TEM pictures. The effective anisotropy constant ($K_{\text{eff}}=1.3 \times 10^5 \text{ J m}^{-3}$) is more than two times higher than the magnetocrystalline value of bulk bcc iron ($K_{\text{MC}}=4.8 \times 10^4 \text{ J m}^{-3}$). Due to the weak value of θ , this increase is rather attributed to size reduction effects¹⁴ than to the presence of magnetic interactions.

Hyperthermia measurements were performed on samples where a large majority of the NPs are located in aggregates, displaying hydrodynamic radii r larger than 250 nm. The Brownian frequency f_B of these agglomerates, calculated using $f_B=k_B T/4\pi\eta r^3$, where $\eta=0.69 \times 10^{-3} \text{ kg m}^{-1} \text{ s}^{-1}$ is the viscosity coefficient of the solvent, leads to $f_B=240$ Hz. Therefore, the agglomerates, and thus the NPs inside them, can be regarded as fixed in the range of 2–300 kHz. Consequently, the losses observed cannot be explained by the mechanical rotation of the NPs themselves (Brownian relaxation) but rather by the reversal of the magnetization inside the NPs.

Figure 3 shows that below a field of $\mu_0 H=30$ mT, the SAR dependence as a function of $\mu_0 H$ follows a square law, in agreement with the LRT for superparamagnetic particles.¹⁵ However, for $\mu_0 H$ above 30 mT, the SAR rises according to a power law with an exponent of 3.2, in disagreement with the LRT model. To explain this deviation above a certain magnetic field, two hypotheses can be put forward: (i) the high magnetic field part is out of the domain of validity of the LRT and/or (ii) the magnetic interactions influence too much the response of the system. With respect to the first hypothesis, the LRT is expected to be valid for magnetically independent NPs only when $\mu_0 H M_S V/k_B T < 1$ (this is the condition for which a Langevin function is linear with the magnetic field) This condition leads precisely to $\mu_0 H < 30$ mT. As a consequence, the LRT model is no longer valid above this limit.

This article shows that 5.5 nm iron NPs have an anisotropy higher than the one of the bulk and do not display maximized hyperthermia properties. Similar studies on larger NPs will constitute the future of this work.

ACKNOWLEDGMENTS

We acknowledge InNaBioSanté foundation, AO3 program from Université Paul Sabatier (Toulouse) and Conseil Régional de Midi-Pyrénées for the financial support, V. Collière (TEMSCAN) for TEM, C. Crouzet for the technical assistance, and A. Mari for magnetic measurements.

- ¹M. Brzeska, M. Panhorst, P. B. Kamp, J. Schotter, G. Reiss, A. Pühler, A. Becker, and H. Brückl, *J. Biotechnol.* **112**, 25 (2004).
- ²A. Ito, M. Shinkai, H. Honda, and T. Kobayashi, *J. Biosci. Bioeng.* **100**, 1 (2005).
- ³R. Hergt and S. Dutz, *J. Magn. Magn. Mater.* **311**, 187 (2007).
- ⁴G. Reiss, H. Brueckl, A. Huettner, J. Schotter, M. Brzeska, M. Panhorst, D. Sudfeld, A. Becker, P. B. Kamp, A. Puehler, K. Wojcizkowski, and P. Jutzi, *J. Mater. Res.* **20**, 3294 (2005).
- ⁵L.-M. Lacroix, R. Bel Malaki, J. Carrey, S. Lachaize, M. Respaud, G. F. Goya, and B. Chaudret, *J. Appl. Phys.* **105**, 023911 (2009).
- ⁶F. Dumestre, B. Chaudret, C. Amiens, P. Renaud, and P. Fejes, *Science* **303**, 821 (2004).
- ⁷L.-M. Lacroix, S. Lachaize, A. Falqui, M. Respaud, and B. Chaudret, *J. Am. Chem. Soc.* **131**, 549 (2009).
- ⁸E. Snoeck, C. Gatel, L. M. Lacroix, T. Blon, S. Lachaize, J. Carrey, M. Respaud, and B. Chaudret, *Nano Lett.* **8**, 4293 (2008).
- ⁹L.-M. Lacroix, S. Lachaize, A. Falqui, T. Blon, J. Carrey, M. Respaud, F. Dumestre, C. Amiens, O. Margeat, and B. Chaudret, P. Lecante and E. Snoeck, *J. Appl. Phys.* **103**, 07D521 (2008).
- ¹⁰E. C. Stoner and E. P. Wohlfarth, *Philos. Trans. R. Soc. London, Ser. A* **240A**, 599 (1948).
- ¹¹J. I. Gittleman, B. Abeles, and S. Bozowski, *Phys. Rev. B* **9**, 3891 (1974).
- ¹²L.-M. Lacroix, J. Carrey, and M. Respaud, *Rev. Sci. Instrum.* **79**, 093909 (2008).
- ¹³J. L. Dormann, F. D’Orazio, F. Lucari, E. Tronc, P. Prené, J. P. Jolivet, R. Cherkaoui, and M. Noguès, *Phys. Rev. B* **53**, 14291 (1996).
- ¹⁴F. Bødker, S. Mørup, and S. Linderoth, *Phys. Rev. Lett.* **72**, 282 (1994).
- ¹⁵R. E. Rosensweig, *J. Magn. Magn. Mater.* **252**, 370 (2002).